Characterizing phase change materials using the T-History method: On the factors influencing the accuracy and precision of the enthalpy-temperature

Citation for the original published paper (version of record):

Tan, P., Brütting, M., Vidi, S. et al (2018). Characterizing phase change materials using the T-History method: On the factors influencing
the accuracy and precision of the enthalpy-temperature curve. Thermochimica Acta, 666: 212-228.
http://dx.doi.org/10.1016/j.tca.2018.07.004

Characterizing phase change materials using the T-History method: On the factors influencing the accuracy and precision of the enthalpy-temperature curve

Pepe Tan[a,1,*], Michael Brütting[b], Stephan Vidi[b], Hans-Peter Ebert[b], Pär Johansson[a], Angela Sasic Kalagasidis[a]

[a] *Department of Architecture and Civil Engineering, Division of Building Technology, Chalmers University of Technology, Gothenburg, Sweden*
[b] *Bavarian Center for Applied Energy Research (ZAE Bayern), Würzburg, Germany*

Abstract

While research on using the latent heat of so called phase change materials (PCMs) for thermal energy storage has gained increasing interest in the last decade, the measurement of its thermal properties are still subject to research. The T-History method has been frequently used by researchers to measure the enthalpy-temperature curve of PCMs but the factors influencing its accuracy and precision have rarely been discussed. This work provides a systematic experimental study of an organic PCM based on different insulated sample holders. It is first shown that the data evaluation method has to be adjusted against noise to improve both accuracy and precision for all experimental setups. The results moreover show that neglecting the insulation thermal mass in the experimental setup leads to systematic errors in the enthalpy results due to oversimplification of the mathematical model. This

*Corresponding author
Email address: pepe.tan@chalmers.se (Pepe Tan)

confirms a previous numerical study by the authors. It is recommended that either the mathematical model or the experimental setup are adjusted in future work to decrease this error. Until then it is generally recommended to use sample holders with a high ratio between the thermal mass of the PCM to the insulated sample holder. This is further supported by a measurement uncertainty analysis via Monte Carlo simulations.

Keywords: Phase Change Materials, Thermal Analysis, Calorimetry, T-History

---

1. Introduction

Utilizing the latent heat of melting and solidification of so called phase change materials (PCMs) has been an active field of research in the last decade, due to the potentially higher energy storage densities compared to sensible storage materials for the same temperature difference [1, 2, 3]. When evaluating a PCM, differential scanning calorimetry (DSC) is typically used to derive the enthalpy versus temperature curve to visualize its phase transition temperature as well as its heat storage potential. However, the small sample sizes in the milligram range used in commercial DSC devices can pose limitations regarding how representable the sample is for the bulk material, especially when measuring heterogeneous materials [3]. Therefore, results from the so called T-History method [4, 5], which utilizes sample sizes in the gram range, have been frequently presented as either an alternative or complementary to DSC measurements [6, 7].

When selecting any measurement method, it is useful to discuss the method with respect to the terms measurement "accuracy" and "precision"

[8]. A measurement is considered as accurate, if the derived value of the measurand is close to it's true value. On the other hand, a measurement is considered as precise or repeatable, if the measurand values of repeated measurements do not show a significant spread [8].

The ideal method therefore should be both precise and accurate. That is, it should be both repeatable and low of systematic errors resulting from the experimental setup and the mathematical model that converts the measured input quantities to the output quantity. For DSC measurements, a recent round robin test has improved both precision and accuracy after defining a common methodology that can be applied across different DSC devices [9]. For the T-History method on the other hand, work is still ongoing to find a suitable experimental setup as well as data evaluation technique [5, 10, 11]. Moreover, recent work has started to critically address the underlying method assumptions [12, 13].

Discussion of the T-History Method assumptions

The T-History method subjects a PCM sample and a reference material to step changes of the ambient temperature within the same controlled environment (typically an air climate chamber). The recorded temperature versus time responses of the PCM sample and reference are then compared to calculate the enthalpy change of the PCM sample based on two major assumptions [14]:

1. It is assumed that the heat flows between the reference material and the ambient $\dot{Q}_{ref}$, and between the PCM and the ambient $\dot{Q}_{PCM}$, are

equal for the same temperature difference $T - T_{amb} = T_{ref} - T_{amb} = T_{PCM} - T_{amb}$:

$$\dot{Q}_{ref}(T) = \dot{Q}_{PCM}(T) = \frac{1}{R_{th}(T)}(T - T_{amb}) \tag{1}$$

2. It is assumed that the measured temperature change over time is representative for the whole sample holder via a lumped model formulation for the sample or reference $k = \{\text{ref}, \text{PCM}\}$ and the sample holder tube:

$$\dot{Q}_k(T) = (m^k \cdot {c_p}^k(T) + m^{tube,k} \cdot {c_p}^{tube}(T)) \cdot \left.\frac{dT}{dt}\right|_k \tag{2}$$

It is important to note that multi-dimensional heat transfer occurs in the actual T-History experiment and that it may be practically difficult to assure one-dimensionality of the heat transfer as well as the uniformity of the temperature profiles in the PCM. Eq. 1 can therefore only be seen as an approximation of the effective heat flux from the sample holders to the ambient. The thermal resistance $R_{th}(T)$ then includes form factors like the overall heat transfer area of the sample holders. A minimum requirement for the first assumption is therefore that the sample holders for PCM and reference are of the same geometrical dimensions. In order to additionally support this assumption, a number of experimental setups previously reported in the literature placed an additional insulation layer around the sample holders [5] making it the dominant component of $R_{th}(T)$.

Previous works using uninsulated sample holders often applied the Biot number criteria $\text{Bi} < 0.1$ in order to support the second assumption. However, it is known that thermal gradients still exist during the experiment

[15, 16]. The thermal gradients can be reduced by either using sample holders with a small diameter or by decreasing the overall heating or cooling rate in the experiment. For the latter, the ambient temperature step change can be decreased and/or the sample holders insulated.

Recent numerical studies done by Mazo et al. 2015 [12] on uninsulated sample holders and by the authors [13] on insulated sample holders have started to critically address the validity of the assumptions in Eq. 1 and 2. Both works relied on simplified 1-dimensional heat transfer simulations by studying the effect of parameter variations of the simulated experiment on the enthalpy versus temperature curve. Both works come to the conclusion that systematic errors are present in the enthalpy results, since Eq. 1 and 2 can only be seen as approximations for the actual transient effects taking place in both the uninsulated and insulated setup since both approaches have certain limitations.

A first deviation in the heat flux is present after the initial ambient temperature step change when the thermal diffusivity of sample and reference are not exactly equal [13].

When the sample holders are uninsulated, the heat flux of sample and reference to the ambient is moreover determined by the heat convection coefficient between the sample holder wall and the ambient. The alternative would be to insulate the sample holders and make R_{th} being dominated by heat conduction through the insulation layer.

In a recent work by Badenhorst & Cabeza 2017 [10], it was shown that the heat convection coefficient may vary largely in an air climate chamber.

Therefore, the assumption of equal thermal resistances may be better supported by using the latter approach, when the experiment is done in these kind of chambers.

In [13], however, systematic errors in the range of up to 4% of the considered enthalpy difference due to neglecting transient effects caused by the thermal mass of the insulation material itself were predicted. The error increased the more insulation thermal mass was present in the setup. A first methodology was also proposed on how to correct the measurement results. However, it was concluded that this error has to be first experimentally confirmed and placed within the context of an overall measurement uncertainty analysis of an actual experiment.

To the best of the authors knowledge, no attempt has been made so far to perform a systematic experimental study regarding the factors that influence both accuracy and precision of the T-History results. Uncertainties of previous experimental studies are usually not reported and these are only based on a single experimental variant. Moreover, details of the data evaluation procedure are usually not fully disclosed.

These kind of studies are however needed to critically assess the validity made in the mathematical model and the experimental setup as well as to confirm the previous numerical work done so far. In this work, the study is based on T-History setups using insulated sample holders. The thermal mass of the insulation is deliberately neglected in Eq. 1 to study experimentally the influence of this assumption in the enthalpy results in analogy to our previous numerical work [13].

1.1. Research objectives

The aim of this work is to improve the T-History method with respect to its accuracy and precision. This is done by identifying and discussing the factors for the experimental setup and the data evaluation which influence the accuracy and repeatability of the enthalpy results.

For this we present an experimental study based on three different T-History setups by using two sample holder and three insulation types. For each T-History setup, the target of the data evaluation method is to yield repeatable results within repetitive measurement cycles for both cooling and heating. The assumptions of equal heat flux and uniform temperature are moreover critically checked for each setup by using three temperature sensors per sample holder and calculating enthalpy curves from each sensor's temperature measurements individually.

A first measure for the accuracy within each setup is then given by the difference between cooling and heating cases. Lastly, if the mathematical model is valid, no differences in the results by changing experimental setup parameters and between the different sensors should be present. However, if differences exist, then this is likely due to systematic errors as mentioned above.

We show that the data evaluation method has to be adjusted individually for cooling and heating in order not to interpret the raw measurement data erroneously. Their influence on the enthalpy calculations are discussed in detail compared to an idealized case.

Furthermore, we perform a study on how estimated input quantity uncertainties (e.g. related to temperature measurements) propagate through the mathematical model and our data evaluation method via Monte Carlo simulations.

2. Material and Methods

2.1. Experimental Setup

The experiments were conducted using cylindrical sample holders, which are made from conventional copper pipes of 10 and 15 mm diameter and 100 mm length (see Fig. 1). Copper is chosen, because it's high thermal conductivity supports the lumped capacity formulation of the sample holder. Additionally, the temperature sensor can be placed directly on the sample holder wall. The sample holders were filled at approximately atmospheric pressure $p \approx 0.1013$MPa with the commercially available paraffin based RT28HC (Rubitherm) as PCM at $T \approx 40$°C and distilled water as reference at $T \approx 20$°C. We refer to other works in the literature that copper may not be compatible with other types of PCMs due to long term corrosion issues [17, 18]. The sample holders are sealed with conventional copper end caps and glue. The sample holders were insulated with different types of closed cell pipe insulations (Armaflex AF) intended for the respective pipe diameter. Due to the geometry of the setup, heat transfer from the sample holder to the ambient is expected to be mostly through the larger cylindrical lateral surface area. The properties of the setups are summarized in Table 1.

The temperature of the sample holders was measured by attaching 10 kOhm thermistors using aluminum tape on the sample holder wall before placing the insulation around the setup. Three thermistors where placed per sample holder along its axial length and denoted as "top", "center" and

Figure 1: Photo of the sample holders used for Setup A (left) and for Setup B1 and 2 (right)

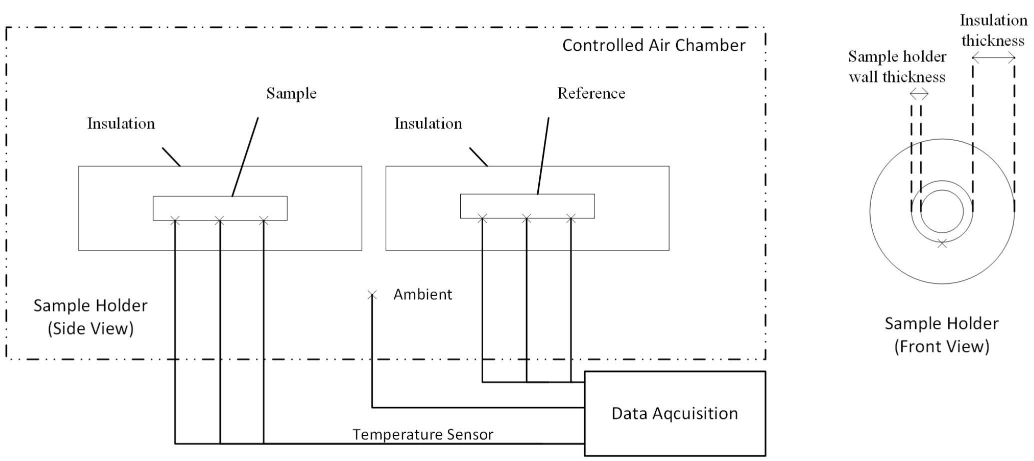

Figure 2: Sketch of the experimental setup. Temperature sensor locations are marked by 'x'.

"bottom" sensor location (see Fig. 2 and 3).

Prior to the experiment, the thermistors were calibrated against a reference thermistor (Fluke 5610-6, traceable expanded $k = 2$ calibration un-

Table 1: Sample holder properties. For setup B1 and B2 the same 15mm sample holder is used but with different insulation types. (Insulation properties are taken from the respective product sheets)

Parameter	Setup A	Setup B1	Setup B2	
Sample holder (outer) diameter	10	15	15	mm
Sample holder length	100	100	100	mm
Insulation type	AF-04-10	AF-04-15	AF-06-15	
Insulation length	150	150	150	mm
Insulation thickness	15.5	17	32	mm
Insulation density	60-80	60-80	60-80	$kg\,m^{-3}$
Insulation thermal conductivity (at 0°C)	0.033	0.033	0.033	$W\,m^{-1}\,K^{-1}$
m^{PCM} (RT28HC, paraffin)	4.2	10.1	10.1	g
m^{ref} (distilled water)	5.4	13.1	13.1	g
$m^{tube,PCM}$	25.2	46.8	46.8	g
$m^{tube,ref}$	25.0	46.9	46.9	g
$R_{th}^{tube} \cdot L$	7.21×10^{-5}	5.92×10^{-5}	5.92×10^{-5}	$m\,K\,W^{-1}$
$R_{th}^{Insulation} \cdot L$	6.61	5.71	8.01	$m\,K\,W^{-1}$

certainty of 0.01 °C plus 0.01 °C due to first-year drift) in the center of a massive aluminum block. The calibration was performed by comparing the thermistors against the reference sensor readings as follows: The sensors were inserted in the aluminum block and the block placed inside a climate chamber (TERCHY MHK408-YK). The temperature in the chamber was increased from 10 to 55 °C in four step changes with enough time (9 hours) for the block and sensors to reach thermal equilibrium after each step change. In a second iteration, the temperature was decreased from 55 to 10 °C in the

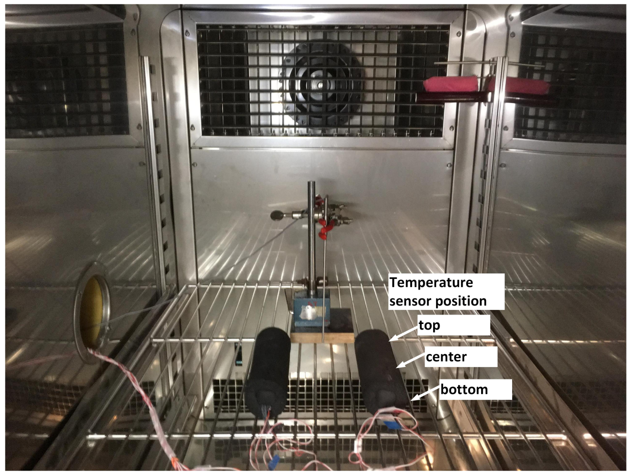

Figure 3: Photo of the experimental setup. All temperature sensors are attached on the underside of the sample holders along its axial length. The "top" sensor is oriented towards the climate chamber fan.

same four steps. We estimate that the fitted coefficients of the Steinhart-Hart resistance to temperature equation using readings from the four temperature steps for each thermistor does not exceed a combined standard uncertainty of $u(T) = 0.1$ °C (expanded uncertainty of $U_c(T) = 0.2$ °C, $k = 2$ (95% level of confidence)).The largest uncertainty contribution was due to the radial temperature uniformity in the aluminum block. The reference thermistor itself was used to record the ambient temperature during the experiments.

Data logging for both calibration and the T-History experiments were performed using the same data acquisition unit (Keysight 34972A with a 16-ch. 34902A multiplexer module).

Each setup was placed centrally inside the above mentioned climate chamber, with the "top" sensor location pointed towards the fan inside the climate chamber (see Fig. 3). The sample holders were placed horizontally in

Table 2: Climate chamber program for setup A and B

Parameter	Program I	Program II	
T_{amb}^{min} - T_{amb}^{max}	$18-38$	$13-43$	°C
$T_{pcm} \pm \Delta T$	28 ± 10	28 ± 15	°C
Duration of one complete heating and cooling cycle	$2 \cdot 12$	$2 \cdot 12$	h
Heating and cooling cycles performed	5	5	
Data acquisition interval	5	5	s

the climate chamber with the temperature sensors facing downwards. The sample holders were then subjected to the two different step temperature programs according to Table 2, representing a higher or lower effective heating and cooling rate. Before the first measurement, the samples were kept at the highest program temperature to ensure that the first solidification starts from a homogenized liquid state. The samples were cycled 5 times to study the repeatability within a single setup and program. The complete experimental study was done over the course of 5 weeks in the following order: B2-I $\rightarrow$ B2-II $\rightarrow$ B1-I $\rightarrow$ B1-II $\rightarrow$ A-I $\rightarrow$ A-II. Since the thermistors where not re-attached during the first four experiments, the results for the B type sample holders are expected to be independent from the goodness of thermal contact between sensor and sample holder wall. The difference in the results are then due to the different levels of insulation and heating/cooling rates.

In addition, three different enthalpy curves are calculated for a single cooling or heating case using the PCM and reference temperature readings from the three sensor locations. This allows an evaluation of the assumption in Eq. 2, that a single temperature sensor is representative for the whole sample holder.

The temperature measurements obtained from the experiments are shown exemplary in Fig. 4 for Setup A-I and A-II. Measurements for the other setups are reported in the supplementary file to this work. A measure for the uniformity of the climate chamber is given by maximum differences of $0.2 - 0.3$°C between all sensors at steady state conditions.

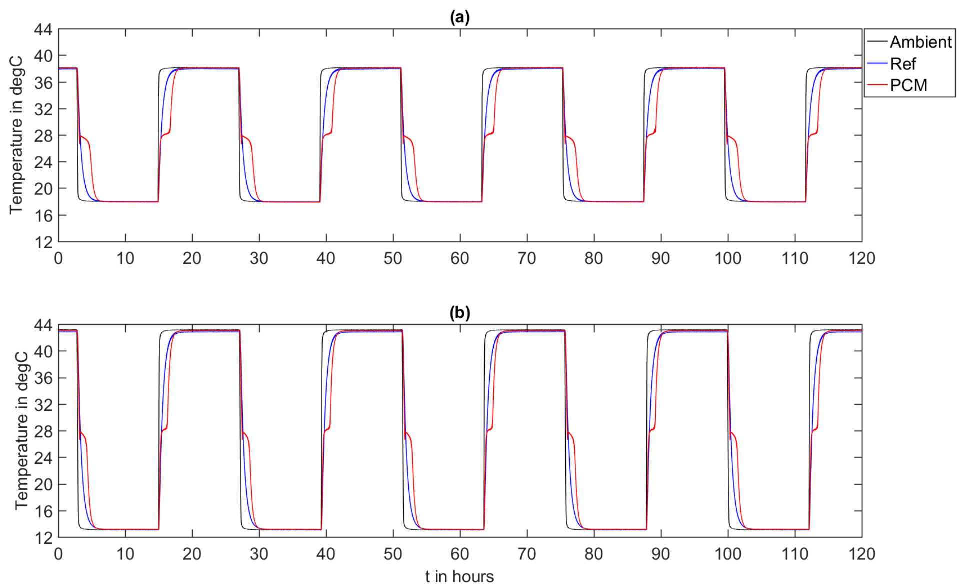

Figure 4: T-History measurements of RT28HC for setup A: (a): A-I, (b): A-II (all three sensor positions for reference and PCM are plotted with the same color, respectively).

2.2. Mathematical model

Enthalpy changes of the PCM can be calculated by combining Eq. 1-2 and solving for the unknown PCM specific heat capacity:

$$c_p{}^{PCM}(T) = \frac{m^{ref} \cdot c_p{}^{ref}(T) + m^{tube,ref} \cdot c_p{}^{tube}(T)}{m^{PCM}} \cdot \frac{\left.\frac{dT}{dt}\right|_{ref}}{\left.\frac{dT}{dt}\right|_{PCM}} - \frac{m^{tube,PCM} \cdot c_p{}^{tube}(T)}{m^{PCM}} \tag{3}$$

For convenience, the terms can be grouped together:

$C_{ref}(T) = \frac{m^{ref} \cdot c_p{}^{ref}(T) + m^{tube,ref} \cdot c_p{}^{tube}(T)}{m^{PCM}}$ and $C_{tube,PCM}(T) = \frac{m^{tube,PCM} \cdot c_p{}^{tube}(T)}{m^{PCM}}$

$$c_p{}^{PCM}(T) = C_{ref}(T) \cdot \frac{\left.\frac{dT}{dt}\right|_{ref}}{\left.\frac{dT}{dt}\right|_{PCM}} - C_{tube,PCM}(T) \tag{4}$$

$$\Delta h^{PCM} = \int_{T}^{T+\Delta T} c_p{}^{PCM}(\tau) d\tau \tag{5}$$

The mathematical expression $\frac{\left.\frac{dT}{dt}\right|_{ref}}{\left.\frac{dT}{dt}\right|_{PCM}}$ in Eq. 4 represents the essential idea of the T-History method: The latent heat of a PCM being calculated by the difference in time it takes for the PCM to undergo the same temperature change compared to a reference, which does not undergo phase change. In alternative formulations, this principle has been expressed in the form of different areas under the temperature versus time curve for the same temperature interval for PCM and reference, respectively [10, 19].

In the following, the data evaluation method is presented on how the enthalpy versus time curve is calculated from the actual measured temperature over time response. We describe necessary simplifications and adjustments in the data evaluation method based on encountered difficulties when using experimental temperature over time data.

2.2.1. Ideal case

In our previous paper [13], the utilization of Eq. 4 from a simulated T-History experiment was straightforward. Only interpolation between temperature and time values was needed in order to express the terms $\left.\frac{dT}{dt}\right|_{ref}$ and $\left.\frac{dT}{dt}\right|_{PCM}$ for the same temperature for both PCM and reference. Interpolation was possible because the simulated temperature vs time curve was in a sense ideal. Because no noise, supercooling or other effects were considered, a strictly monotonically increasing or decreasing temperature curve was obtained with unique $T = f(t)$ values depending on a cooling or heating case. These ideal cases can be defined by the following conditions:

- Cooling: Both reference and PCM temperature curves $T = f(t)$ are strictly monotonically decreasing and their time derivatives are $\left.\frac{dT}{dt}\right|_{PCM} < 0$ and $\left.\frac{dT}{dt}\right|_{ref} < 0$.
- Heating: Both reference and PCM temperature curves $T = f(t)$ are strictly monotonically increasing and their time derivatives are $\left.\frac{dT}{dt}\right|_{PCM} > 0$ and $\left.\frac{dT}{dt}\right|_{ref} > 0$.

The resulting enthalpy curve was then subjected to two major systematic errors due to the limitations of the mathematical model: (1) by neglecting the temperature gradient inside the PCM sample holder due to the lumped model assumption. This is represented via the well known hysteresis of the enthalpy curve between cooling and heating cases [16]. (2) by neglecting the insulation thermal mass. This results in differences in transmittive heat flows at the temperature sensor location, which in turn underestimated the latent heat released and overestimated the effective heat capacity in the sensible parts [13]. The underestimation of the latent heat was by far the most dominant error when evaluating the enthalpy difference across the phase change temperature range. The two errors on the resulting enthalpy curve can be seen as an assignment of the enthalpy value to the wrong temperature or a calculation of a wrong enthalpy value itself, respectively. Since the two errors are systematic, they pose a limit on the achievable accuracy of the T-History method.

2.2.2. Non-ideal cases

For discrete data, the derivatives $\frac{dT}{dt}\Big|_{ref}$ and $\frac{dT}{dt}\Big|_{PCM}$ in Eq. 4 can only be approximated with numerical schemes. In this work we utilize the forward approximation of the derivative:

$$\frac{dT}{dt}(t) = \frac{T(t+\Delta t) - T(t)}{\Delta t} - O(\Delta t) \approx \frac{T(t+\Delta t) - T(t)}{\Delta t} \tag{6}$$

This scheme is first order accurate, since the truncation error $O(\Delta t)$ would decrease direct proportionally with the chosen step length Δt. In the experiment, the smallest possible step length is given by the data acquisition rate of 5s.

Analogous to the forward discretization, temperature intervals can then be directly defined from adjacent discrete PCM data values:

$$\left.\frac{dT^i}{dt}\right|_{PCM} = \frac{T^{i+1}_{PCM} - T^i_{PCM}}{t^{i+1}_{PCM} - t^i_{PCM}} = \frac{T^{i+1}_{PCM} - T^i_{PCM}}{\Delta t^i_{PCM}} \tag{7}$$

In our measurements, the reference temperature curve and its time derivative fulfill the ideal case conditions for both heating and cooling since the reference stores or releases only sensible heat (see Fig. 5). Using the PCM temperature interval it is then possible to interpolate for the reference time values $t^i_{ref} = f^{ref}_{interp}(T^i_{PCM})$ and $t^{i+1}_{ref} = f^{ref}_{interp}(T^{i+1}_{PCM})$. A time derivative based on the PCM temperature interval can then be formulated for the reference:

$$\left.\frac{dT^i}{dt}\right|_{ref} \approx \frac{T^{i+1}_{PCM} - T^i_{PCM}}{t^{i+1}_{ref} - t^i_{ref}} = \frac{T^{i+1}_{PCM} - T^i_{PCM}}{\Delta t^i_{ref}} \tag{8}$$

When formulating the ratio of the time derivatives in Eq. 4, the temperature interval is canceled out and only the time differences remain:

$$\frac{\left.\frac{dT^i}{dt}\right|_{ref}}{\left.\frac{dT^i}{dt}\right|_{PCM}} \approx \frac{\Delta t^i_{PCM}}{\Delta t^i_{ref}} = \frac{t^{i+1}_{PCM} - t^i_{PCM}}{t^{i+1}_{ref} - t^i_{ref}} \tag{9}$$

$$c_p^{PCM}(T^i) = C_{ref}(T^i) \cdot \frac{\Delta t^i_{PCM}}{\Delta t^i_{ref}} - C_{tube,PCM}(T^i) \tag{10}$$

For the PCM, this is also the case within its sensible temperature range. However, during phase change, the temperature curve and its time derivative deviate from the ideal cases for both cooling and heating. This then needs special attention and adjustments in the data evaluation procedure when calculating the enthalpy curve from Eq. 10.

In the following, we list these deviations separately for cooling and heating in order to explain the phenomena behind them and discuss their influence on the accuracy and precision of the enthalpy curve.

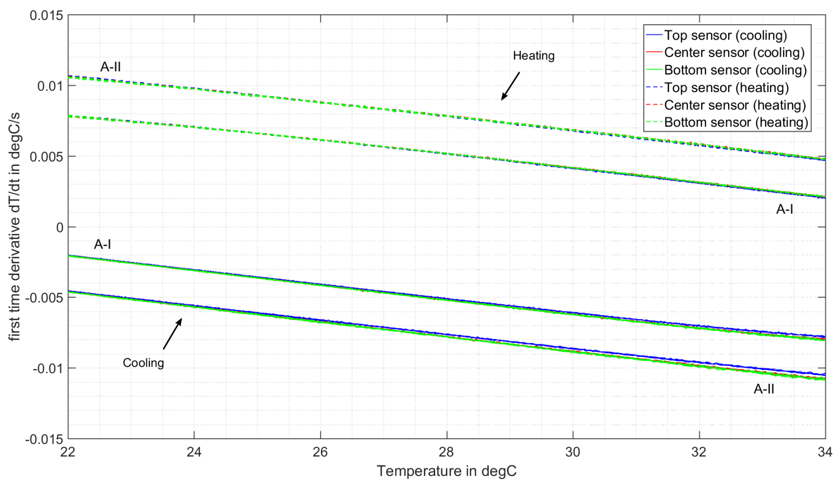

Figure 5: $\left.\frac{dT}{dt}\right|_{ref}$ vs T values for Setup A-I and A-II (sensor data from 5 cycles are plotted with the same color)

Cooling

Fig. 6 shows a typical $\left.\frac{dT}{dt}\right|_{PCM}$ vs T curve for a cooling case. From the figure, the non-ideal conditions can be summarized as:

- $\left.\frac{dT}{dt}\right|_{ref} < 0$, but $\left.\frac{dT}{dt}\right|_{PCM} > 0$; Due to heat release during recalescence from a supercooled state. In Eq. 4, this leads to negative c_p^{PCM} values.
- $\left.\frac{dT}{dt}\right|_{PCM} = 0$; Balance of heat release during recalescence and heat loss to ambient, or due to random noise and a too high data recording rate. In Eq. 4, this leads to $c_p^{PCM} \to \infty$.

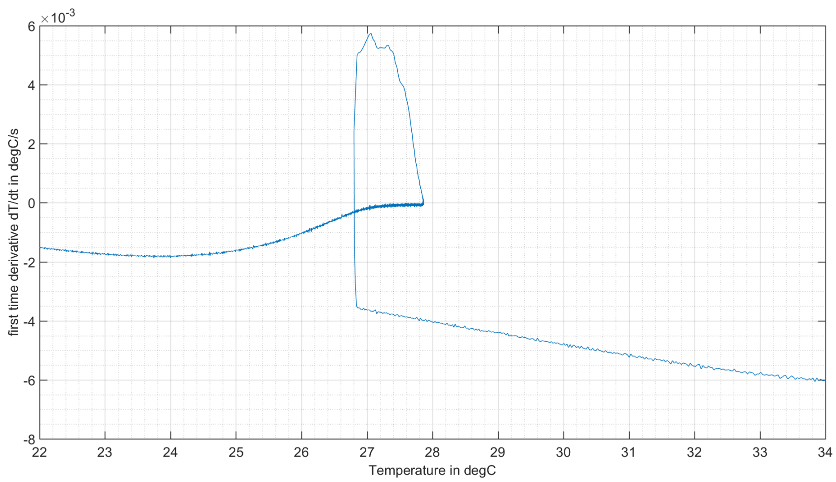

Figure 6: Example of $\left.\frac{dT}{dt}\right|_{PCM}$ vs T values for Setup B2-I (top sensor, cooling cycle 1)

During cooling, the PCM curve has values $\left.\frac{dT}{dt}\right|_{PCM} > 0$ due to the sudden heat release caused by recalescence (see Fig. 6). That is when the supercooled liquid rapidly solidifies. It is obvious that these derivative values can not be inserted directly into Eq. 4, since they would yield a negative heat capacity $c_p^{PCM}(T) < 0$, which has no physical meaning. What has been proposed in a recent work is to use absolute values for $\left|\frac{\left.\frac{dT}{dt}\right|_{ref}}{\left.\frac{dT}{dt}\right|_{PCM}}\right|$ [11], which has also been adopted by our algorithm by setting $\frac{\left|\Delta t^i_{PCM}\right|}{\left|\Delta t^i_{ref}\right|}$ in Eq. 10. However, a systematic error is likely introduced, since then it is assumed that the heat flows are equal for a reference cooling case and a PCM heating case.

In our experiments, it was moreover observed that using absolute values for the derivative still leads to negative heat capacity values. This is because during recalescence $C_{ref}(T) \cdot \left|\frac{\left.\frac{dT}{dt}\right|_{ref}}{\left.\frac{dT}{dt}\right|_{PCM}}\right| < C_{tube,PCM}(T)$ holds in Eq. 4, since $\left.\frac{dT}{dt}\right|_{PCM}$ in the denominator is larger compared to $\left.\frac{dT}{dt}\right|_{ref}$. For these cases, we propose to set the negative heat capacity values to $c_p^{PCM} := 0$, which essentially means that the onset of recalescence is assumed to be adiabatic.

This simplification can be justified due to the existing insulation around the sample holders and if the degree of supercooling is small. In all of our experiments, the same degree of approx. 1°C supercooling was observed.

In the cooling curve, a singularity $\left.\frac{dT}{dt}\right|_{PCM} = 0$ can moreover occur, e.g. when the heat release during the final stages of recalescence from supercooling is in balance with the heat loss to the ambient. It would then not be possible to evaluate Eq. 4 directly since $c_p^{PCM}(T) \to \infty$. This problem was already mentioned previously in [20].

A way to circumvent the singularity is to define a minimum allowed evaluation step size dT and to compare it with the recorded discrete temperature versus time data within a flexible evaluation window T^i_{PCM}, $T^{i+\Delta i}_{PCM}$.

The window size Δi is forced to increase $\Delta i := \Delta i + 1$ when the condition $\left|T_{PCM}^{i+\Delta i} - T_{PCM}^{i}\right| \geq dT$ is not fulfilled, following the idea of Stankovic 2014 [21, 22]. If dT is chosen as very small, the evaluation window size will be $\Delta i = 1$ most of the time, leading to the standard forward difference scheme using the immediate neighboring discrete data (at $\Delta t = 5$s data acquisition rate). However, any singularities $T_{PCM}^{i} = T_{PCM}^{i+1}$ are circumvented at the cost that the calculated derivative is then calculated from a larger step size $t_{PCM}^{i+\Delta i} - t_{PCM}^{i}$ due to the increased evaluation window $\Delta i > 1$:

$$\frac{dT^i}{dt}\bigg|_{PCM} = \frac{T_{PCM}^{i+\Delta i} - T_{PCM}^{i}}{t_{PCM}^{i+\Delta i} - t_{PCM}^{i}} \tag{11}$$

On the other hand, if a large dT is chosen, the T vs t curve is essentially smoothed out. A trade off therefore has to be found when choosing the evaluation step dT.

Another observed problem is the fixed data acquisition rate and the thermal response time of the temperature sensor itself during recalescence. If the original data in Fig. 7 were used, then the heat capacity would be overestimated due to the apparent low temperature change at the beginning of recalescence (visible as an apparent plateau in the figure). In reality, the onset of recalescence likely lies at a lower temperature in between the apparent plateau. In order to make the data evaluation more robust against these cases, the data point and its adjacent values are skipped. This problem should be avoided in future experiments by using temperature sensors with a faster response time and a faster data recording rate.

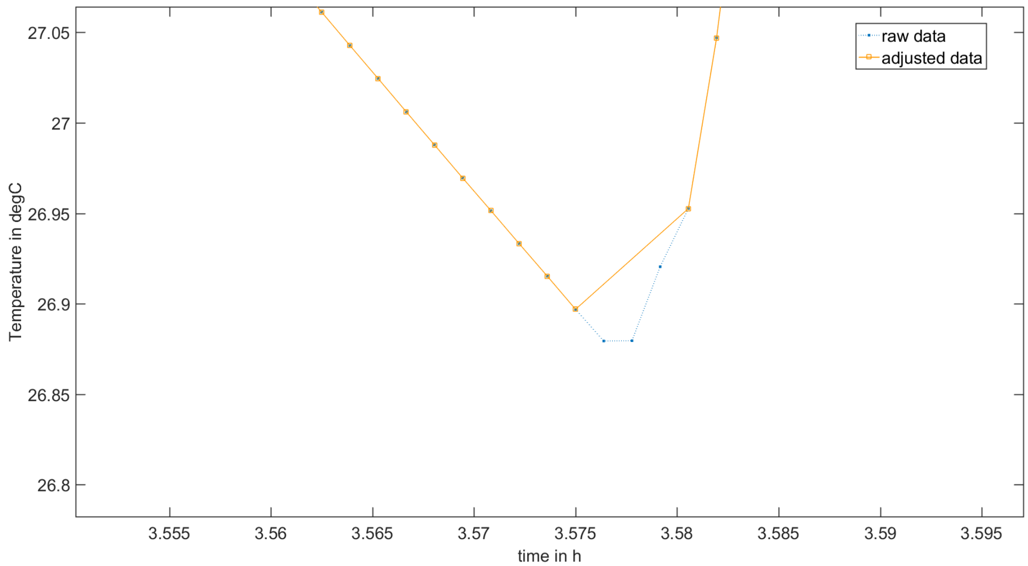

Figure 7: Example of adjustment made for the PCM sample cooling curve to avoid overestimating the specific heat capacity during recalescence (B2-I, 2nd cooling cycle, bottom sensor)

From Figure 4 it can be seen that the PCM apparently solidifies over a wider temperature range compared to the melting curve. An explanation for this can be found in an increasing heat transfer resistance between the sensor location and the solidification front, which progresses from the sensor position towards the center of the sample holder [3]. Due to this heat conduction dominated process, little apparent temperature fluctuations are measured and the time derivative is $\frac{dT}{dt}\Big|_{PCM} < 0$ for the remaining cooling part after recalescence, which makes the treatment of the differentials more straight forward compared to the heating curve once a suitable value for dT has been determined. This in turn means that the precision of the cooling curve is mainly limited by how reproducible the temperature recording of the different sensors is for subsequent cycles. It seems plausible to assume that this can be subject to a certain randomness depending at which location inside the sample holder the PCM starts solidifying and how the solidification front progresses.

The accuracy in turn should be mainly limited by systematic errors in the mathematical model given by the discussed problems during supercooling, neglecting the insulation thermal mass and by assuming that a single temperature sensor is representative for the whole sample holder.

Heating

Fig. 8 shows a typical $\frac{dT}{dt}\Big|_{PCM}$ vs T curve for a heating case. From the figure, the non-ideal conditions can be summarized as:

- $\frac{dT}{dt}\Big|_{ref} > 0$, but $\frac{dT}{dt}\Big|_{PCM} \leq 0$ in the form of pronounced "noise" due to natural convection, especially towards the end of melting

In contrast to the cooling curve, all temperature sensors recorded strong temperature fluctuations over the entire melting duration (which we define as apparent "noise" subsequently) in the PCM sample holder. Since we observed that these fluctuations are especially pronounced during the later stages of melting, it is likely that natural convection is occurring within the sample holder. The noise can then be explained by the notion that the initially formed liquid phase at the sample holder wall is heating up faster, while the remaining solid phase stays at the phase change temperature. When more liquid phase forms and heats up at the sample holder wall, the solid phase becomes smaller and is increasingly subjected to the convective flows

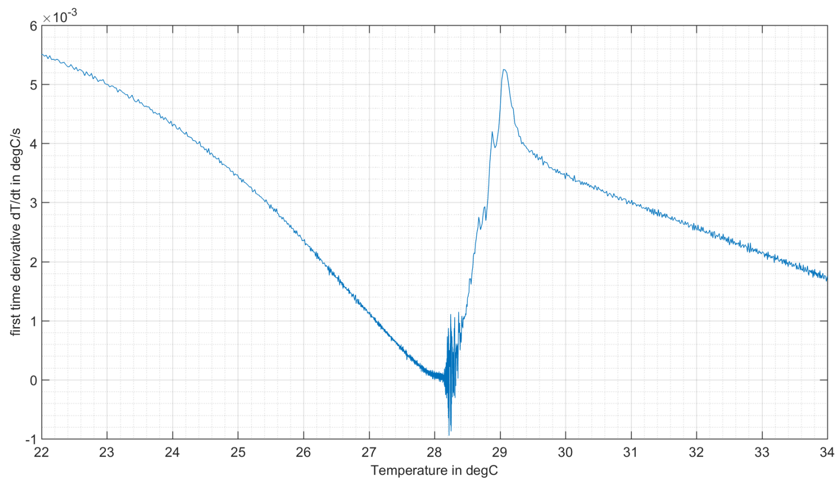

Figure 8: Example of $\left.\frac{dT}{dt}\right|_{PCM}$ vs T values for Setup B2-I (top sensor, heating cycle 1)

occurring in the liquid phase. It is likely that this is more pronounced with increasing differences in densities between the solid and liquid phase.

Any movement between solid and liquid phases of different temperatures at the temperature sensor location cause the sensor to record these fluctuations as apparent noise due to the high thermal conductivity of the copper sample holder and our high data sampling rate.

The fact that melting of the PCM is observed to be faster than solidification in our experiments, despite the similar temperature difference between ambient and phase change temperature, also supports that natural convection is present, since it is known to reduce the melting time. If only conductive heat transfer would be present during melting, a shorter solidification time compared to melting would be expected since the thermal conductivity is known to be significantly larger in the solid phase for paraffins such as n-octadecane [23], which RT28HC is likely based on.

Because natural convection has already been discussed even for small DSC sample sizes [24], it is likely that the phenomenon is even more pronounced in the larger T-History samples.

The apparent noisy temperature data has a direct influence on the time derivative of the PCM melting curve $\frac{dT}{dt}\Big|_{PCM}$, which changes between positive $\frac{dT}{dt}\Big|_{PCM} > 0$ and negative values $\frac{dT}{dt}\Big|_{PCM} < 0$ during melting. Due to the randomness, there are also cases where singularities $\frac{dT}{dt}\Big|_{PCM} = 0$ can be present in the time derivative leading to the same problem as discussed above for cooling.

When the temperature versus time curve is noisy, it contributes to both under and overestimations of the PCM specific heat capacity. Apparent rapid temperature changes are e.g. interpreted as "reduced" heat capacity and enthalpy changes by the mathematical model. On the other hand, random noise may also artificially lower the calculated value of $\frac{dT}{dt}\Big|_{PCM}$ leading to an overestimation of the heat capacity and enthalpy change (similar to the previous example of Fig. 7 for cooling cases).

Moreover, since noise is amplified when differentiating, the value of $\frac{dT}{dt}\Big|_{PCM}$ itself becomes distorted (see Fig. 8) and the noisy derivative values can not be simply inserted into Eq. 4.

In any of our experimental setups, the existence of natural convection in the form of noise has therefore a pronounced influence on both accuracy and precision of the method when the enthalpy is calculated from the heating case. The evaluation of $\frac{dT}{dt}\Big|_{PCM}$ then turns into a signal conditioning problem, where a derivative has to be reconstructed from noisy data. In signal processing, it is well known that differentiation of noisy data is not a trivial problem [25, 26]. A compromise has to be therefore made when formulating the data evaluation method.

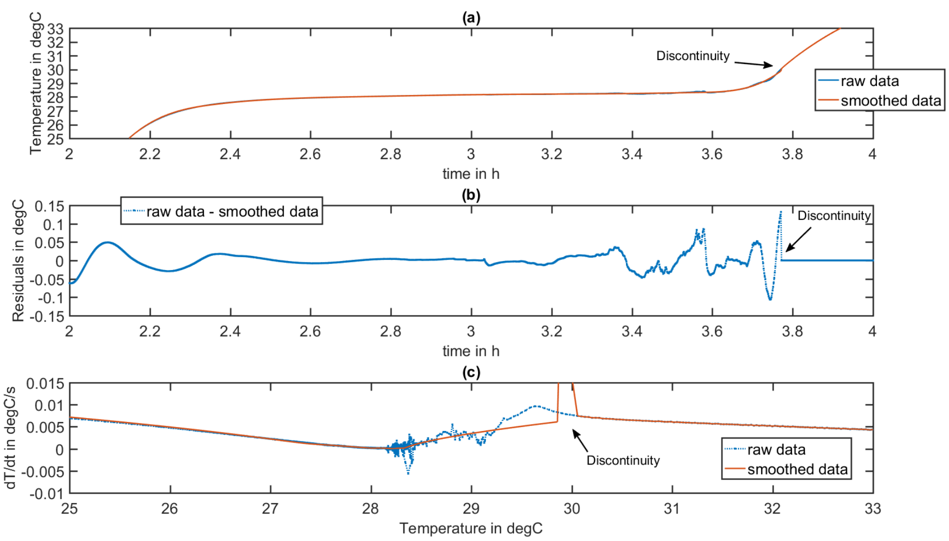

Figure 9: Example of smoothing the PCM sample heating curve (A-I, 1st heating cycle, top sensor) using the SLM toolbox: (a): T vs. t, (b): Residuals $= T_{raw} - T_{smooth}$ vs. t, (c): $\left.\frac{dT}{dt}\right|_{PCM}$ vs. T (The discontinuity at $T = 30$°C is because smoothing is only performed until $T < 30$°C and then the original data is used.)

One approach is to smoothen the original T versus t curve itself. This should be done with care, since smoothing manipulates the original data and a bias trough the user is introduced. There is also the risk that intrinsic behavior of the PCM is overwritten. Moreover, signal smoothing can be done in a variety of ways [26].

In this work, we propose to perform smoothing based on the previously formulated conditions of an ideal heating curve. The noisy temperature over time data is then smoothened out by fitting a strictly monotonous increasing spline for all heating curves in this work. For this, the MATLAB based Shape Language Modeling (SLM) toolbox by D'Errico [27] is utilized. Once the spline has been applied, no further adjustments are necessary since the derivative of the smoothed curve is $\left.\frac{dT}{dt}\right|_{PCM} > 0$ for the entire range (e.g. see Fig. 9). In order not to over-smooth the sensible regions, the spline is applied only until $T < 30$°C. For $T > 30$°C, the original data is used. This causes a discontinuity in the derivative $\left.\frac{dT}{dt}\right|_{PCM}$ and an underestimation of the heat capacity in the transition between smoothed and original data. Since this is only over a small temperature difference of two data points and within the sensible region, the error in the overall enthalpy curve is negligible.

It will be seen later via the resulting enthalpy curves that smoothing the data significantly improves the precision and overall accuracy since random high frequency noise is smoothed out and the overall time derivative for $\left.\frac{dT}{dt}\right|_{PCM}$ can be approximated in a consistent way. However, it comes at the cost that the systematic error introduced by smoothing the data itself is unknown.

2.2.3. Algorithm

The above discussed details for cooling and heating cases are then implemented into a data evaluation algorithm in MATLAB v2016b. The algorithm is summarized as pseudo code in Fig. 10. The temperature dependent heat capacities for water and copper are given by functional expressions of the temperature formulated in [28] and [29], respectively. However, in the actual T-History experiment the exact pressure p and $u(p)$ is unknown inside the PCM and reference sample holder. Using temperature dependent isobaric specific heat capacities formulated near atmospheric pressure can therefore only be seen as an estimate, which introduces additional systematic errors.

Fig. 11 shows the evaluation temperature intervals for three different dT values for a cooling case. As mentioned above, if a very small dT is chosen, essentially the original raw data points are used to calculate the enthalpy. When forming the derivative as shown in Fig. 12, it can be seen that the derivative of the raw data points are noisy especially in the region where the temperature versus time curve has its plateau. Similar to heating, it is likely that the enthalpy curve is being distorted as well when it is calculated from the original noisy derivative. It can be seen that choosing a larger dT essentially smooths out the differential and yields a more plausible enthalpy curve in Fig. 13, while using the noisy derivatives appears to yield an over-estimation of the enthalpy curve. Since there was only little difference in the enthalpy curve between $dT = 0.01$°C and $dT = 0.001$°C, the latter is chosen, since this step length approximated the temperature versus time curve better as seen in Fig. 11.

For heating, the fitted spline over the noisy T versus t data intrinsically yields a smooth derivative and the enthalpy results are therefore more robust from a chosen dT value (see Fig. 14).

let $i := 1, \Delta i := 1$;

let $T^{i}_{PCM}, T^{i+\Delta i}_{PCM} \in \Big[T_{min}, T_{max}\Big]^{eval}$;

if *"Heating Case"* **then**

  perform SLM smoothing;

else

  skip recalescence values;

end

repeat

  if $\Big|T^{i+\Delta i}_{PCM} - T^{i}_{PCM}\Big| \geq dT$ **then**

    $\Delta t^{i}_{PCM} = t^{i+\Delta i}_{PCM} - t^{i}_{PCM}$;

    $\Delta t^{i}_{ref} = f^{ref}_{interp}(T^{i+\Delta i}_{PCM}) - f^{ref}_{interp}(T^{i}_{PCM})$;

    $c_p^{PCM}(T^i) = C_{ref}(T^i) \cdot \frac{\left|\Delta t^{i}_{PCM}\right|}{\left|\Delta t^{i}_{ref}\right|} - C_{tube,PCM}(T^i)$;

    if $c_p^{PCM}(T^i) < 0$ **then**

      let $c_p^{PCM}(T^i) := 0$;

    end

    $\Delta h^{PCM}(T^i) = \int_{T^i}^{T^{i+\Delta i}} c_p^{PCM}(\tau) d\tau$;

    let $i := i + \Delta i$;

    let $\Delta i := 1$;

  else

    let $\Delta i := \Delta i + 1$;

  end

until $T^{i}_{PCM}, T^{i+\Delta i}_{PCM} \notin \Big[T_{min}, T_{max}\Big]^{eval}$;

Figure 10: Pseudo code to calculate enthalpy values from discrete data using a flexible temperature window size and absolute $\frac{\left|\Delta t_{PCM}\right|}{\left|\Delta t_{ref}\right|}$ values.

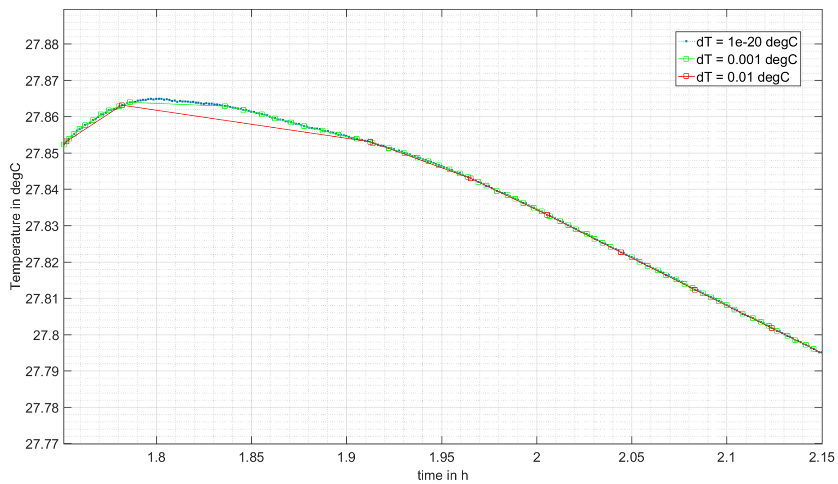

Figure 11: Example of T_{PCM} vs t values using different minimum evaluation step sizes dT for Setup B2-I (top sensor, cooling cycle 1)

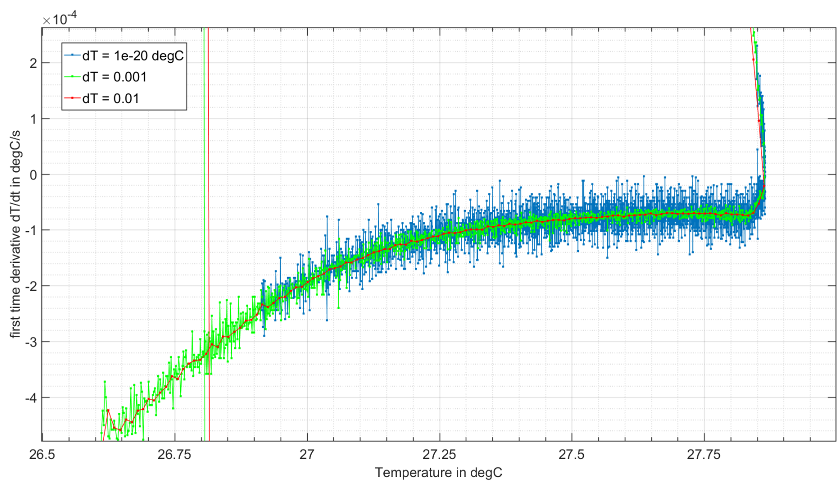

Figure 12: Example of $\left.\frac{dT}{dt}\right|_{PCM}$ vs T values using different minimum evaluation step sizes dT for Setup B2-I (top sensor, cooling cycle 1)

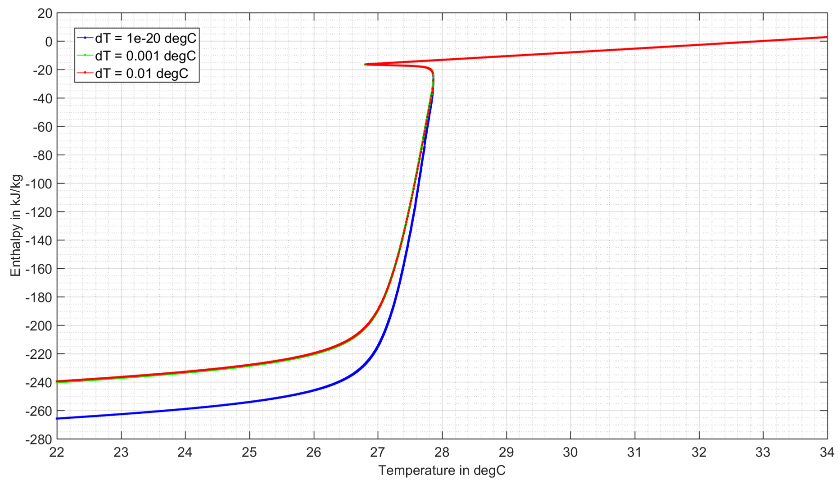

Figure 13: Example of h vs T values using different minimum evaluation step sizes dT for Setup B2-I (top sensor, cooling cycle 1, normalization of h values at 33°C)

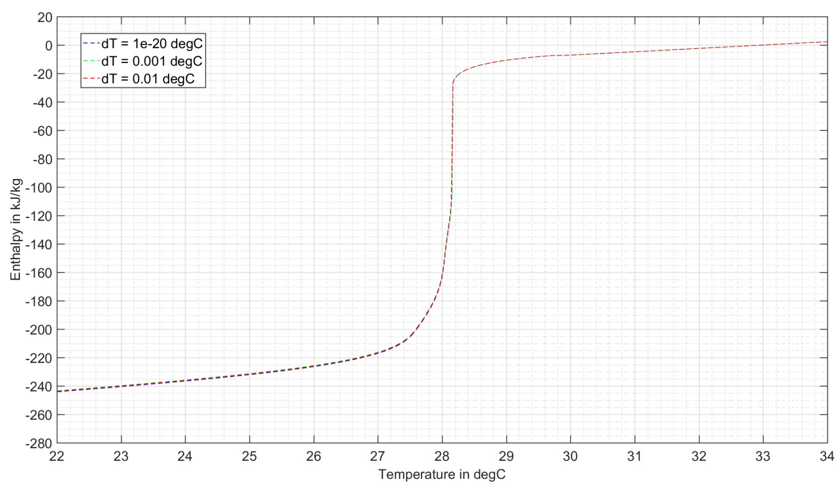

Figure 14: Example of h vs T values using different minimum evaluation step sizes dT for Setup B2-I (top sensor, heating cycle 1, normalization of h values at 33°C)

3. Results & Discussion

3.1. Enthalpy curves

For each experimental setup, the data evaluation algorithm from Fig. 10 is applied for the evaluation window of $[22°\text{C}, 34°\text{C}]^{eval}$ and a chosen minimum temperature step interval of $dT = 0.001°\text{C}$. Examples for enthalpy curves for each sensor location and heating and cooling cycle are shown for the climate chamber program I in Fig. 17-19. The mean enthalpy difference over the temperature interval of $33-23°\text{C}$ (with a combined standard uncertainty of $u(T) = 0.1\text{K}$ for the temperature sensors) and the standard deviation over the five repeated heating and cooling cycles are shown in Fig. 15-16. In total, 30 enthalpy curves are calculated for each experimental setup. However, systematic deviations appear to be present when comparing the results among the different setups.

Setup A yields a systematically smaller enthalpy value compared to setup B1 and B2. This is likely due to the smaller sample size with the same level of insulation compared to B1 and B2. This is in agreement with the prediction of our previous simulation study that the larger the present thermal mass of the insulation is with respect to the sample size, the larger the systematic underestimation of the enthalpy [13]. However, the enthalpy shift of setup B2 with respect to B1 on average appears to be not significant when compared to the limits of repeatability within repetitive cycles. Since it was shown that systematic errors are observable, it can be concluded that the transient heat transfer effects due to the insulation thermal mass should not have been neglected in this experimental setup.

The precision of the enthalpy value for each sensor location over the five cycles is acceptable since the largest standard deviation in any setup was found to be ≤ 1.25 kJ kg^{-1}. This is mainly due the performed smoothing of the heating curve and by choosing dT carefully for the cooling curve. It is likely that the good repeatability is a direct result of insulating the sample holders, which dominates the heat transfer in the experiments.

Moreover, the enthalpy values between cooling and heating cases appear to be consistent within < 5 kJ kg^{-1}.

It can be seen that the top sensor located towards the fan generally estimates a lower enthalpy value compared to the center and bottom sensor locations. Since this is valid for all setups, it is likely that the cause for this is the climate chamber fan itself causing the top part of the PCM sample to cool down or heat up faster compared to the top part of the reference.

Concerning the hysteresis between cooling and heating cases, it can be concluded that in general the larger temperature step change of program II leads to a larger hysteresis, compared to program I, regardless of the setup. A complete figure of the enthalpy plots can be found in the supplementary file for this paper. This observation is in analogy with DSC measurements, that the overall lower heating or cooling rate leads to smaller temperature gradients inside the sample [9, 16]. It can also be seen that setup A yields a smaller hysteresis compared to setup B1, due to the smaller diameter of the sample holders in A. However, the hysteresis can be also decreased with a thicker layer of insulation in setup B2. Moreover, the enthalpy shift to lower values is then not as pronounced as in setup A. Therefore, setup B2-I appears to be a good trade off between a desired low hysteresis ($\Delta T_{melting-solid.} \leq 1$°C) and a low error by neglecting the insulation thermal mass.

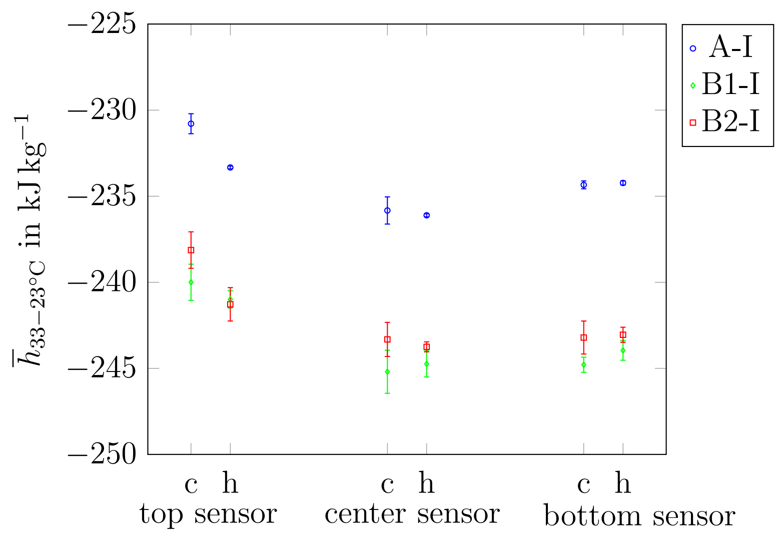

Figure 15: Mean enthalpy results and standard deviation for Setup A-I, B1-I and B2-I over five cycles for each sensor location (c: cooling, h: heating).

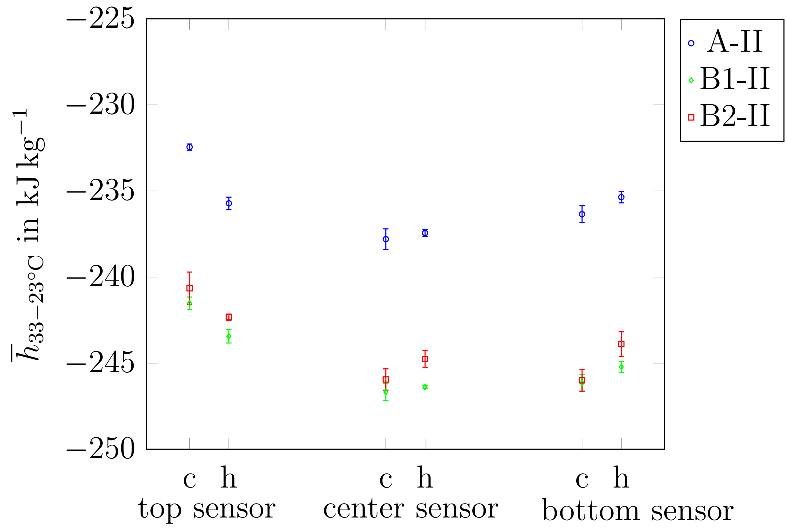

Figure 16: Mean enthalpy values and standard deviation for Setup A-II, B1-II and B2-II over five cycles for each sensor location (c: cooling, h: heating).

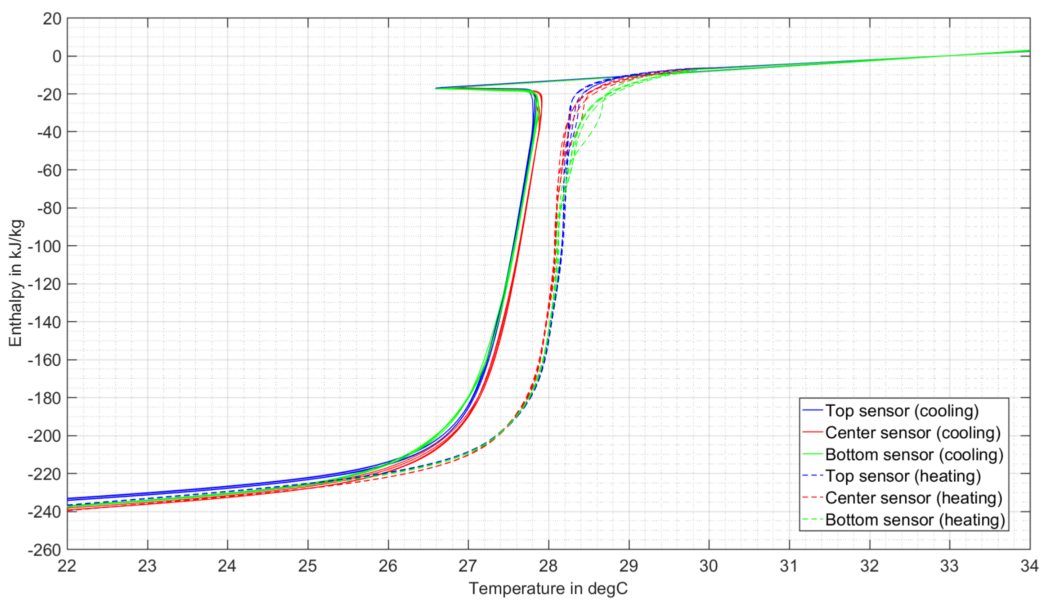

Figure 17: h versus T curve for setup A-I using $dT = 0.001°C$ (all five cycles are plotted with the same color depending on the sensor position, normalization of h values at 33°C)

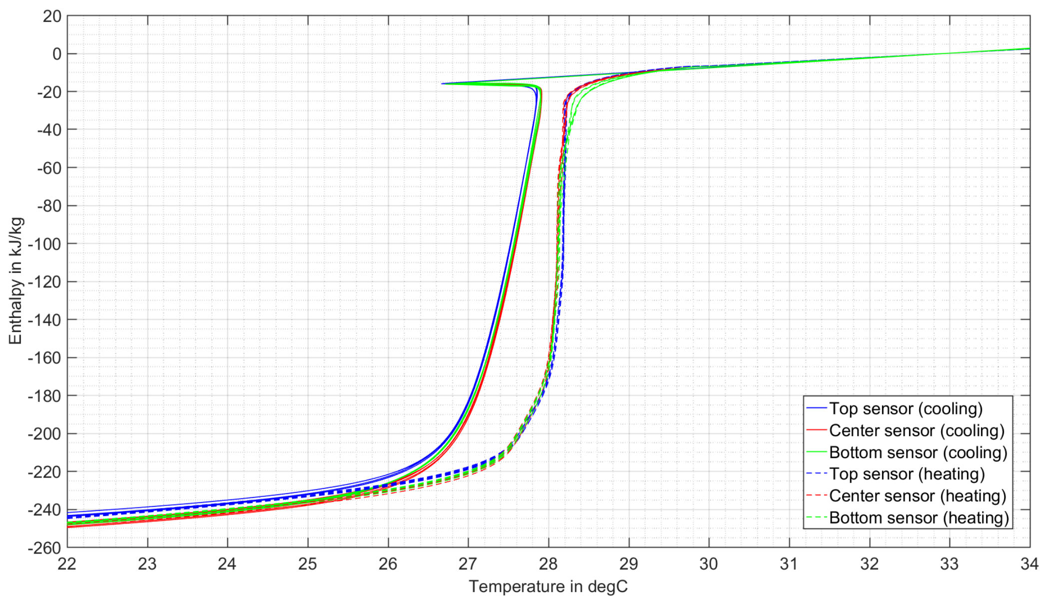

Figure 18: h versus T curve for setup B1-I using $dT = 0.001$°C (all five cycles are plotted with the same color depending on the sensor position, normalization of h values at 33°C)

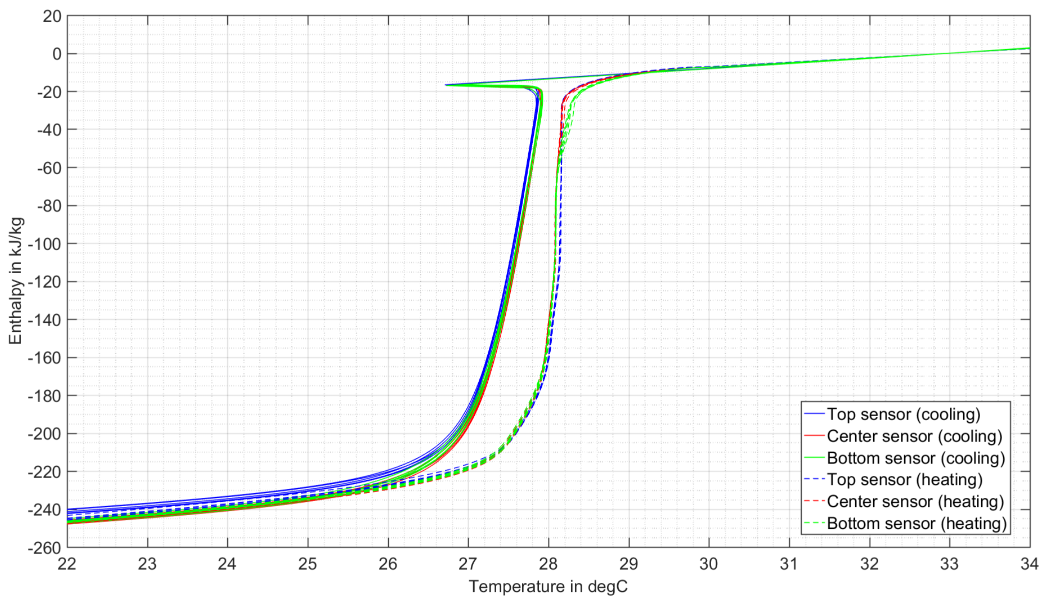

Figure 19: h versus T curve for setup B2-I using $dT = 0.001$°C (all five cycles are plotted with the same color depending on the sensor position, normalization of h values at 33°C)

It can be seen that the enthalpy value is in good agreement with the manufacturers data sheet shown in Fig. 20 ($h_{33-23°C} \approx -237$ to -243.5 kJ kg^{-1}) obtained using a so called three-layer calorimeter. The measurement principle resembles the T-History method [30, 31]. However, no further details on experimental parameters and data evaluation method are given.

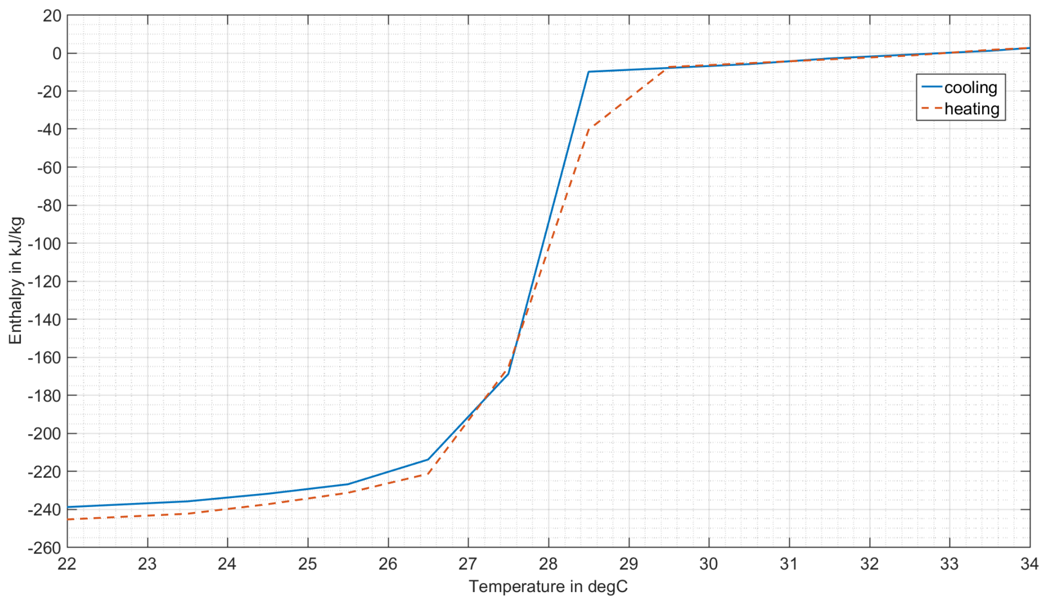

Figure 20: h versus T curve plotted from the manufacturer's data sheet [32] (normalization of h values at 33°C). (Cooling: $h_{33-23°C} = -237$ kJ kg^{-1}, Heating: $h_{33-23°C} = -243.5$ kJ kg^{-1})

3.2. Solid and liquid specific heat capacities

The mathematical model of the T-History method also allows an evaluation of the liquid and solid specific heat capacity of the PCM. From Eq. 1 and 2 an expression for c_p^{PCM} can be derived in the liquid and solid regions:

$$(m^{PCM} \cdot {c_p}^{PCM}(T) + m^{tube,PCM} \cdot {c_p}^{tube}(T)) \cdot \left.\frac{dT}{dt}\right|_{PCM} = \frac{1}{R_{th}(T)}(T_{PCM} - T_{amb}) \tag{12}$$

$$\left.\frac{dT}{dt}\right|_{PCM} = \frac{1}{R_{th}(T) \cdot (m^{PCM} \cdot {c_p}^{PCM}(T) + m^{tube,PCM} \cdot {c_p}^{tube}(T))}(T_{PCM} - T_{amb}) \tag{13}$$

When Eq. 13 is evaluated over a small temperature difference in the sensible regions, the temperature dependence of the terms may be neglected. Then it may be assumed that a linear relationship between $\left.\frac{dT}{dt}\right|_{PCM}$ and T_{PCM} should hold:

$$\left.\frac{dT}{dt}\right|_{PCM} \approx K \cdot (T_{PCM} - T_{amb}) \tag{14}$$

However from Fig. 21 and 22 it can be seen that a linear relationship in the sensible parts does not hold for the PCM or reference in the solid region for a heating case and in the liquid region for a cooling case, which mark the beginning of the experiment. This is likely because the mathematical model does not account for the initial heat flux with the present insulation directly after the step change of T_{amb}. This phenomenon was shown in the previous simulation study [13]. Therefore, $c_{p,s}^{PCM}$ and $c_{p,l}^{PCM}$ are evaluated as mean value from the $dT = 0.001$°C steps within the marked temperature interval close to T_{amb}. $c_{p,s}^{PCM}$ is calculated from the cooling curve within

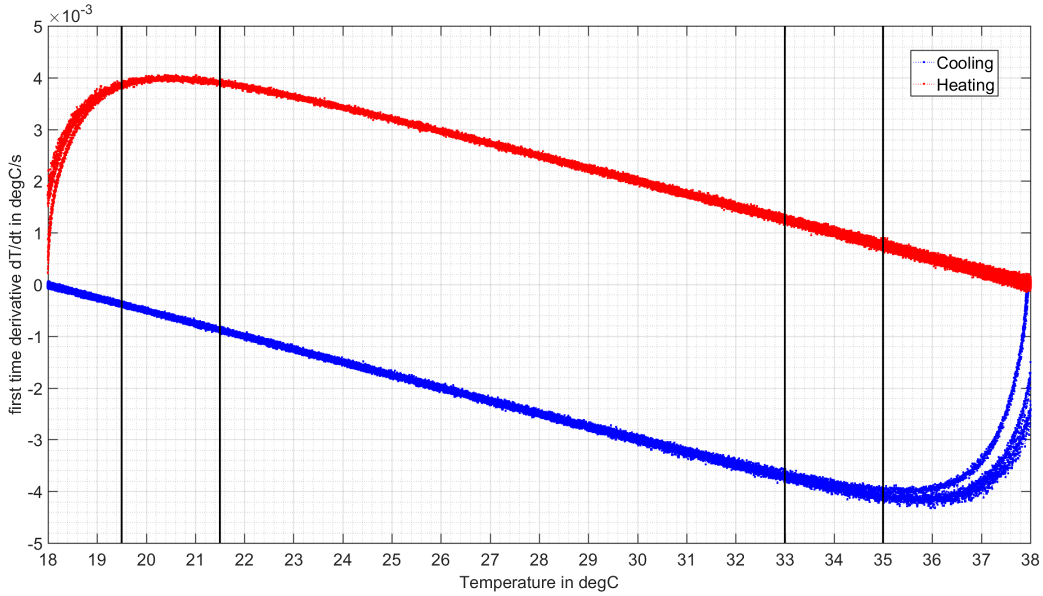

Figure 21: $\frac{dT}{dt}\Big|_{ref}$ versus T curve for setup B2-I (all sensor positions and cycles are plotted with the same color depending on heating or cooling)

$[19.5°\text{C},\ 21.5°\text{C}]^{eval}$ and $c_{p,l}^{PCM}$ from the heating curve within $[33°\text{C},\ 35°\text{C}]^{eval}$.

The results in Fig. 23-24 indicate that both liquid and solid heat capacities are overestimated compared to the specified $2\ \text{kJ}\,\text{kg}^{-1}\,\text{K}^{-1}$ for solid and liquid c_p^{PCM} by the manufacturer (no information about the corresponding temperature range and its uncertainty is given) [32]. This is because the assumption of equal heat flux is likely only valid if the thermal diffusivity of both sample and reference are identical [13]. If not, also the heat capacities in the sensible region need to be systematically corrected when the insulation thermal mass is neglected as shown in our previous work [13].

On a positive note, the standard deviations for repeated cycles are very low (2.5×10^{-3} to 28.9×10^{-3} $\text{kJ}\,\text{kg}^{-1}\,\text{K}^{-1}$), showing a very good precision

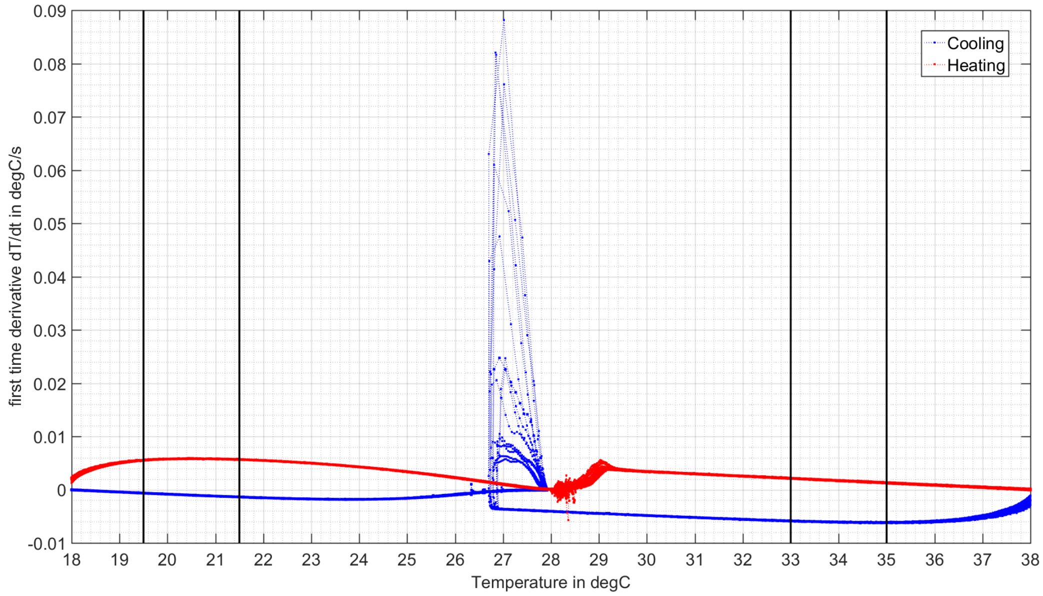

Figure 22: $\left.\frac{dT}{dt}\right|_{PCM}$ versus T curve for setup B2-I (all sensor positions and cycles are plotted with the same color depending on heating or cooling)

of the method. The exact values are given in the supplementary file.

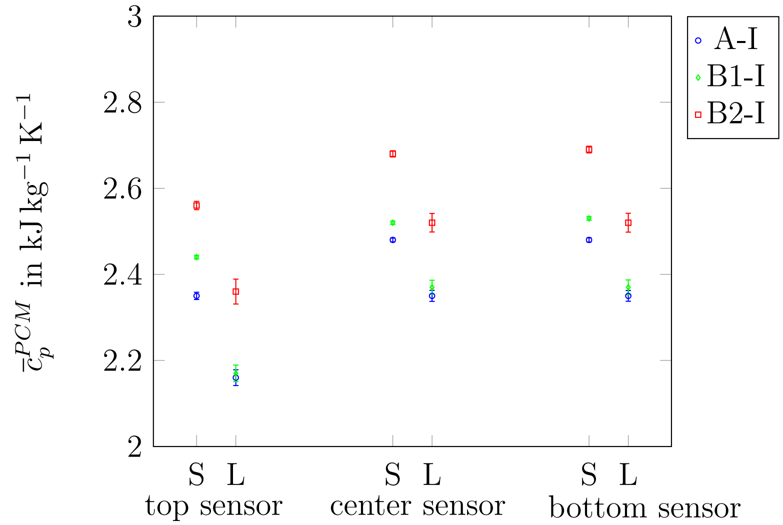

Figure 23: Mean specific heat capacity and standard deviation for Setup A-I, B1-I and B2-I over five cycles for each sensor location (S: solid phase, L: liquid phase).

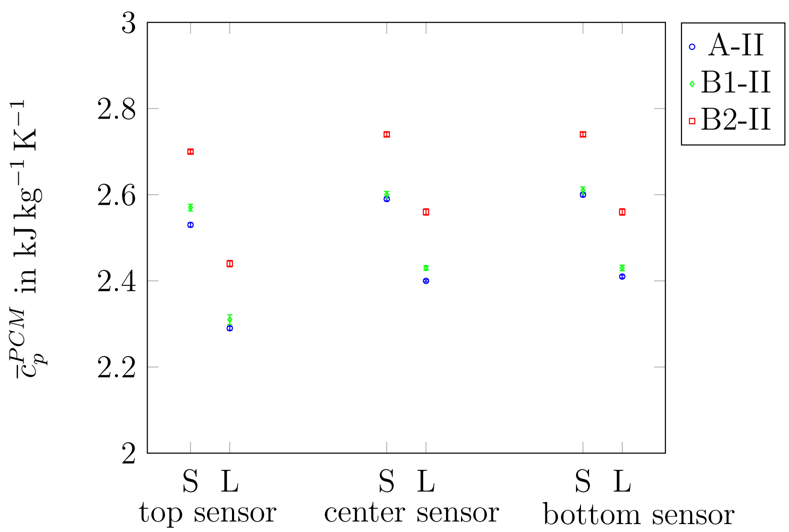

Figure 24: Mean specific heat capacity and standard deviation for Setup A-II, B1-II and B2-II over five cycles for each sensor location (S: solid phase, L: liquid phase).

3.3. Estimation of propagation of input quantity probability density functions (PDF's)

In addition to the enthalpy results, we evaluate how the uncertainty of the enthalpy values are related to uncertainties in the other input parameters (such as temperature, mass and specific heat capacity) in Eq. 3. Since the mathematical model is non-linear and the data evaluation method applies further adjustments to the raw data, a measurement uncertainty analysis is not straightforward. For such cases, the Joint Committee for Guides in Metrology (JCGM) recommends to apply Monte Carlo simulations [33]. This method allows the estimation of propagation of uncertainties of the input quantities X_i to the output quantity Y, for any functional relationship between them:

$$Y = f(X_1, X_2, ..., X_N) \tag{15}$$

For T-History, input quantities are the parameters given in Eq. 3 (see Fig. 25 as illustration). The output quantity is the enthalpy value for a given temperature obtained by the functional relationship of the above discussed data evaluation algorithm in Fig. 10.

In this part we utilize the Monte Carlo methodology described in the Guide to the Expression of Uncertainty in Measurement (GUM), to estimate how the probability density functions (PDF's) of the input quantities in Eq. 3 propagate through the enthalpy calculation algorithm. We assume that all input quantities follow their distribution assigned in Table 3. Considering the experimental temperature range, Arblaster 2015 [29] specifies the copper specific heat capacity for two temperature regions and their respective stan-

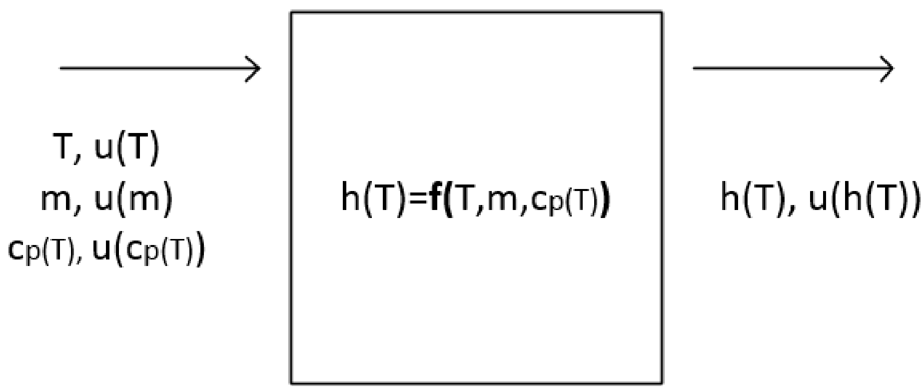

Figure 25: Illustration of the propagation of PDF's according to GUM [33]

dard deviations. As simplification and conservative estimate, we assign the highest relative standard deviation (0.1%) to both regions.

For this study, in every Monte Carlo trial, a value for each input quantity is drawn from its assigned distribution using MATLAB's Marsenne Twister random number generator. We assume that the complete temperature data for each cooling or heating case to be shifted by a single value drawn from the temperature PDF, given by the calibration standard uncertainty.

As a compromise between reliability of the generated random numbers and the computation time, the Monte Carlo simulation is performed $100,000$ times and the results are shown as box plots in Fig. 26 - 27. The number of trials was determined as enough for this study, since the difference in results using lower trials were below the chosen number of significant digits (1kJ/kg) for the enthalpy value $h_{33-23°\mathrm{C}}$. The study was performed for setup A-I, B1-I

Table 3: Assignment of PDF's to input quantities of Eq. 3

Input Quantity	Assigned PDF	PDF Parameter	Source
T	normal	$u(T) = 0.1°\mathrm{C}$	Combined standard uncertainty from calibration.
m^{ref}, m^{PCM}, $m^{tube,ref}$, $m^{tube,PCM}$	rect.	Lower and upper limits: $m \pm 0.1\mathrm{g}$	Estimated from scale specification.
$c_p^{ref}(T)$	normal	$u_r(c_p^{ref}) = 0.05\%$	relative standard uncertainty for pure liquid water at $p = 0.1\mathrm{MPa}$ and $253.15\mathrm{K} \leq T \leq 383.15\mathrm{K}$ from [28][a]
$c_p^{tube}(T)$	normal	$u_r(c_p^{tube}) = 0.1\%$	relative standard uncertainty for pure solid copper at $300\mathrm{K} \leq T \leq 1357.77\mathrm{K}$ from [29][a]

[a] Since in the T-History experiment p and $u(p)$ is unknown inside the PCM and reference sample holder the actual uncertainties for the isobaric specific heat capacities may be higher than in this table.

and B2-I using the first cooling and heating cycle of the center sensor.

The whiskers for setup A-I extend to about $\pm 20\ \mathrm{kJ\,kg^{-1}}$ from the median, while they extend to only $\pm 12\ \mathrm{kJ\,kg^{-1}}$ for setup B1-I and B2-I. This is likely because of the smaller ratio of PCM sample- to insulation- and sample holder tube thermal mass in setup A compared to setup B, while the absolute input quantity uncertainties is unchanged in the Monte Carlo study. Moreover, the spread of the enthalpy results are larger compared to the deviations between the different sensor positions or the standard deviation within repeated cycles. To decrease the uncertainty of the enthalpy results, a future focus should therefore be to decrease the uncertainty of the input quantities.

Therefore, it is recommended that future T-History experiments should be done with as accurate mass and temperature measurements as possible.

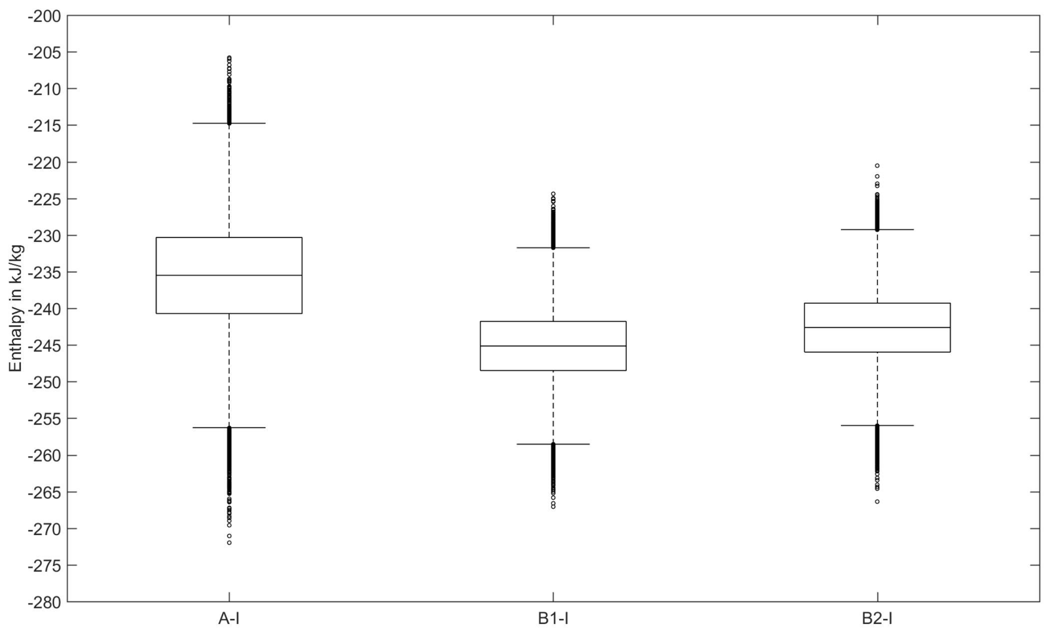

Figure 26: Box plots of $h_{33-23^{\circ}\mathrm{C}}$ values from Monte Carlo simulations for setup A-I, B1-I and B2-I using $dT = 0.001^{\circ}$C (center sensor position, cooling cycle 1). Whiskers are extended to 1.5 times the interquartile range (IQR) [34]

Regarding the sample holder, it is moreover recommended to increase the ratio of PCM sample thermal mass to insulation and sample holder tube thermal masses, in order to dampen the uncertainty on the enthalpy output quantity depending on the same input quantity uncertainties.

4. Conclusions & Future work

In this work the T-History method has been studied by performing repeated measurements using different experimental setups.

When deriving enthalpy values from the mathematical model using the ratio of first time derivatives from the PCM and reference temperature read-

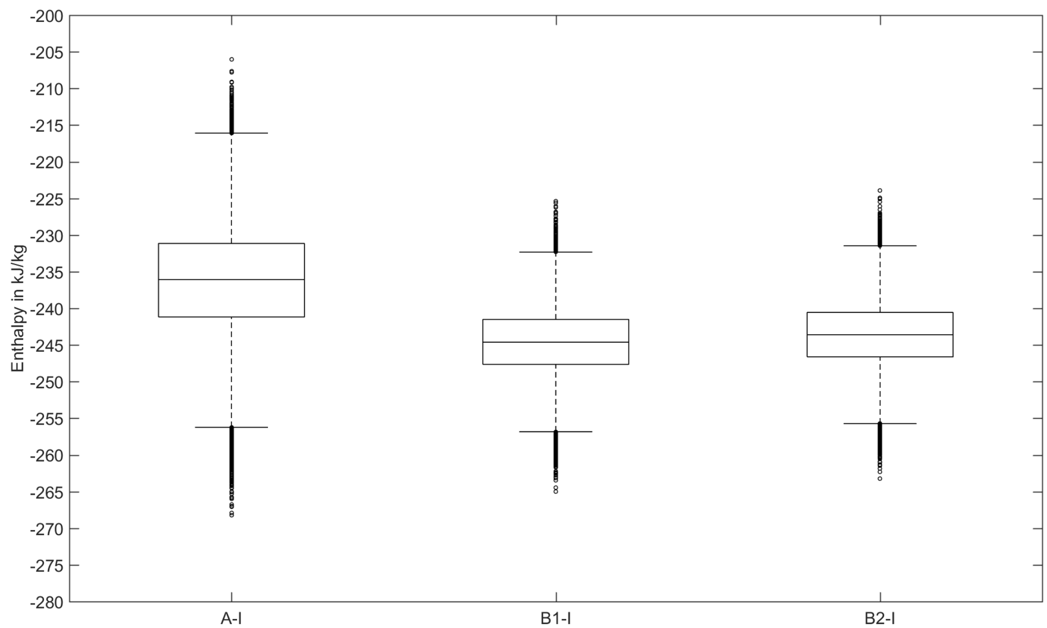

Figure 27: Box plots of $h_{33-23°\mathrm{C}}$ values from Monte Carlo simulations for setup A-I, B1-I and B2-I using $dT = 0.001°\mathrm{C}$ (center sensor position, heating cycle 1). Whiskers are extended to 1.5 times the interquartile range (IQR) [34]

ings, special care has to be taken that noisy data are not interpreted as apparent small or large specific heat capacities. This is especially true, since noise is enhanced when differentiating. It was shown that several adjustments in the data evaluation method were necessary in order to obtain a good enough precision for repetitive measurements within all experimental setups. A consistent data evaluation method is therefore a minimum requirement for discussing other systematic errors present.

However, the data evaluation methodology itself likely introduces to a certain degree systematic errors, such as the proposed smoothing procedure. It is also expected that the applied method is more valid for PCM's with a small degree of supercooling.

Nevertheless, the experimental setup used in this study retained its simplicity, while being able to achieve repeatable results for the apparent enthalpy curves of melting and solidification.

It was shown that in order to approximate the phase change temperature between the apparent melting and solidification curves, the thermal gradients inside the PCM sample should be decreased. This can be done by either decreasing the sample holder diameter or by increasing the degree of insulation leading to smaller overall heating or cooling rates in the experiment. With the current assumptions, one has to be aware that the systematic error due to neglecting the transient heat transfer effects in the insulation is then increased as a trade-off to a lower hysteresis.

Three experimental variants were used to show that the influence of the thermal mass of the insulation material on the enthalpy values appears to be significant on top of the other considered phenomena. The systematic shift to lower enthalpy values with a larger insulation thermal mass ratio (with respect to the PCM sample thermal mass) therefore supports the prediction made by our previous work [13]. Among the setups used in this work, setup B2-I yielded a good trade-off between a low hysteresis and the error of neglecting the insulation thermal mass compared to the other alternatives. However, it is still clear that future setups, which use insulated sample holders and at the same time Eq. 1 as a mathematical basis, have to either decrease the thermal mass of the insulation or subsequently correct the results. An alternative would be to start from a new mathematical basis, which intrinsically accounts for the insulation.

Monte Carlo simulations for T-History experiments have been moreover introduced as one way to estimate how the different input quantity uncertainties propagate through the data evaluation algorithm resulting in a spread of the enthalpy values representing the uncertainty of the results. From this study it can be recommended that the experimental setup should provide a high PCM thermal mass with respect to the sample holder tube. This means that the uncertainty propagation of input quantities are dampened with respect to the PCM results in the mathematical model. This also means that setup B2-I is preferable compared to the smaller sample holder diameter of setup A. In future work, this technique should be developed further to incorporate possible correlations of the input quantity uncertainties. Moreover, the robustness of the method should be tested using a higher number of Monte Carlo trials. For a more rigorous analysis, such as the calculation of confidence intervals, the adaptive Monte Carlo method given by [33, 35] may be implemented in future work. The method can also be used to study the influence of each uncertainty by itself, such as the temperature sensor accuracy, to determine which input quantity uncertainty should be decreased primarily.

Finally, we believe that Monte Carlo simulations can also be used by other researchers on their own T-History variants leading to an overall improvement of the method by providing more insight to their measurement setups and data evaluation method. These simulations can also be used in future work, when applying correction or calibration factors to minimize all systematic errors in the final results. Then the uncertainty related to these factors itself could be propagated.

It is necessary for future work to compare the limits of accuracy and precision of the insulated experimental setup in this work with the predicted errors on the enthalpy results by Mazo et al. 2015 [12] and Badenhorst & Cabeza 2017 [10] using uninsulated sample holder setups.

In general, more work is needed to quantify and reduce the systematic errors stemming from the experimental setup and the current assumptions of the T-History method. This also includes using expressions for the isobaric specific heat capacity c_p^{ref} and c_p^{tube} from the literature to calculate the enthalpy of the PCM, while the actual pressure inside the sample holder over the course of the experiment is unknown. The latter likely depends also on the thermal expansion of the reference material and PCM over the temperature range of the experiment. In order to validate the results from T-History setups, future work should focus on performing round robin tests on a PCM with well documented properties, such as a pure substance.

The experimental raw data of this work is provided by the authors as additional supplementary material to the article.

Acknowledgments

This work was carried out as part of the first author's PhD studies. The funding provided by the Swedish Energy Agency (Energimyndigheten) and the Swedish Centre for Innovation and Quality in the Built Environment (IQ

Samhällsbyggnad) within the E2B2 program is gratefully acknowledged. The authors also thank the Swedish Environmental Protection Agency (Naturvårdsverket) and the Chalmers Energy Area of Advance, Profile area: Energy in Urban Development for the additional financial support.

Nomenclature

$\dot{Q}$	Heat flux (W)
σ_i	Standard deviation of quantity i
c_p	Specific heat capacity ($\mathrm{J\,kg^{-1}\,K^{-1}}$)
h	Specific enthalpy ($\mathrm{J\,kg^{-1}}$)
m	Mass (kg)
R_{th}	Thermal resistance ($\mathrm{K\,W^{-1}}$)
T	Temperature (°C)
t	Time (s)
$u(i)$	Standard uncertainty of quantity i
$U_c(i)$	Combined expanded uncertainty of quantity i
$u_r(i)$	Relative standard uncertainty of quantity i
amb	Ambient
PCM	Phase change material
ref	Reference material
$tube$	Sample holder tube

References

[1] B. Zalba, J. M. Marín, L. F. Cabeza, H. Mehling, Review on thermal energy storage with phase change: materials, heat transfer analysis and applications, Applied Thermal Engineering 23 (3) (2003) 251–283. doi:10.1016/S1359-4311(02)00192-8.

[2] T. Kousksou, P. Bruel, A. Jamil, T. El Rhafiki, Y. Zeraouli, Energy storage: Applications and challenges, Solar Energy Materials and Solar Cells 120 (2014) 59–80. doi:10.1016/j.solmat.2013.08.015.

[3] H. Mehling, L. F. Cabeza, Heat and cold storage with PCM: An up to date introduction into basics and applications; with 28 tables, Heat and Mass Transfer, Springer, 2008.

[4] Y. Zhang, Y. Jiang, Y. Jiang, A simple method, the T-history method, of determining the heat of fusion, specific heat and thermal conductivity of phase-change materials, Measurement Science and Technology 10 (3) (1999) 201.

[5] A. Solé, L. Miró, C. Barreneche, I. Martorell, L. F. Cabeza, Review of the T-history method to determine thermophysical properties of phase change materials (PCM), Renewable and Sustainable Energy Reviews 26 (2013) 425–436. doi:10.1016/j.rser.2013.05.066.

[6] C. Rathgeber, H. Schmit, L. Miró, L. F. Cabeza, A. Gutiérrez, S. Ushak, S. Hiebler, A. Hauer, Analysis of supercooling of phase change materials with increased sample size – Comparison of measurements via DSC, T-

History and at pilot plant scale, in: Greenstock 2015 - 13th IEA ECES Conference.

[7] C. Rathgeber, H. Schmit, P. Hennemann, S. Hiebler, Calibration of a T-History calorimeter to measure enthalpy curves of phase change materials in the temperature range from 40 to 200 C, Measurement Science and Technology 25 (3) (2014) 35011. doi:10.1088/0957-0233/25/3/035011.

[8] Joint Committee for Guides in Metrology, International Vocabulary of Metrology – Basic and General Concepts and Associated Terms: JCGM 200:2012.

[9] S. Gschwander, T. Haussmann, G. Hagelstein, A. Solé, L. F. Cabeza, G. Diarce, W. Hohenauer, D. Lager, A. Ristic, C. Rathgeber, P. Hennemann, H. Mehling, C. Penalosa, A. Lazaro, Standardization of PCM Characterization via DSC, in: Greenstock 2015, 2015.

[10] H. Badenhorst, L. F. Cabeza, Critical analysis of the T-history method: A fundamental approach, Thermochimica Acta-doi:10.1016/j.tca.2017.02.005.

[11] K. D'Avignon, Modeling and Experimental Validation of the Performance of Phase Change Material Storage Tanks in Buildings, PhD thesis (2015).

[12] J. Mazo, M. Delgado, A. Lazaro, P. Dolado, C. Pe?alosa, Marin J. M., B. Zalba, A theoretical study on the accuracy of the T-history method for enthalpy-temperature curve measurement: analysis of the influence of thermal gradients inside T-history samples, Measurement

Science and Technology 26 (12) (2015) 125001. doi:10.1088/0957-0233/26/12/125001.

[13] P. Tan, M. Brütting, S. Vidi, H.-P. Ebert, P. Johansson, H. Jansson, A. S. Kalagasidis, Correction of the enthalpy–temperature curve of phase change materials obtained from the T-History method based on a transient heat conduction model, International Journal of Heat and Mass Transfer 105 (2017) 573–588. doi:10.1016/j.ijheatmasstransfer.2016.10.001.

[14] S. Hiebler, Kalorimetrische Methoden zur Bestimmung der Enthalpie von Latentwärmespeichermaterialien während des Phasenübergangs: (in German), PhD thesis, TUM (2007).

[15] H. Hong, S. K. Kim, Y.-S. Kim, Accuracy improvement of T-history method for measuring heat of fusion of various materials, International Journal of Refrigeration 27 (4) (2004) 360–366. doi:10.1016/j.ijrefrig.2003.12.006.

[16] E. Günther, S. Hiebler, H. Mehling, R. Redlich, Enthalpy of Phase Change Materials as a Function of Temperature: Required Accuracy and Suitable Measurement Methods, International Journal of Thermophysics 30 (4) (2009) 1257–1269. doi:10.1007/s10765-009-0641-z.
URL `http://dx.doi.org/10.1007/s10765-009-0641-z`

[17] A. Solé, L. Miró, C. Barreneche, I. Martorell, L. F. Cabeza, Corrosion of metals and salt hydrates used for thermochemical energy storage, Renewable Energy 75 (2015) 519–523. doi:10.1016/j.renene.2014.09.059.

[18] S. Ushak, P. Marín, Y. Galazutdinova, L. F. Cabeza, M. M. Farid, M. Grágeda, Compatibility of materials for macroencapsulation of inorganic phase change materials: Experimental corrosion study, Applied Thermal Engineering 107 (2016) 410–419. doi:10.1016/j.applthermaleng.2016.06.171.

[19] J. M. Marín, B. Zalba, L. F. Cabeza, H. Mehling, Determination of enthalpy temperature curves of phase change materials with the temperature-history method: improvement to temperature dependent properties, Measurement Science and Technology 14 (2) (2003) 184–189. doi:10.1088/0957-0233/14/2/305.

[20] L. Moreno-Alvarez, J. N. Herrera, C. Meneses-Fabian, A differential formulation of the T-History calorimetric method, Measurement Science and Technology 21 (12) (2010) 127001. doi:10.1088/0957-0233/21/12/127001.

[21] S. B. Stanković, P. A. Kyriacou, Improved measurement technique for the characterization of organic and inorganic phase change materials using the T-history method, Applied Energy 109 (2013) 433–440. doi:10.1016/j.apenergy.2013.01.079.

[22] S. Stankovic, Investigation of advanced experimental and computational techniques for behavioural characterisation of phase change materials (pcms), PhD thesis, City University London (2014).
URL `http://openaccess.city.ac.uk/3671/`

[23] C. Vélez, M. Khayet, J. M. Ortiz de Zárate, Temperature-dependent

thermal properties of solid/liquid phase change even-numbered n-alkanes: N-Hexadecane, n-octadecane and n-eicosane, Applied Energy 143 (2015) 383–394. doi:10.1016/j.apenergy.2015.01.054.

[24] D. David, K. Johannes, F. Kuznik, Quantification of the natural convection perturbations on differential scanning calorimetry measurements of PCMs, Thermochimica Actadoi:10.1016/j.tca.2017.06.004.

[25] J. J. Stickel, Data smoothing and numerical differentiation by a regularization method, Computers & Chemical Engineering 34 (4) (2010) 467–475. doi:10.1016/j.compchemeng.2009.10.007.

[26] P. H. C. Eilers, A Perfect Smoother, Analytical Chemistry 75 (14) (2003) 3631–3636. doi:10.1021/ac034173t.

[27] J. D'Errico, SLM - Shape Language Modeling.
URL https://se.mathworks.com/matlabcentral/fileexchange/

[28] J. Pátek, J. Hrubý, J. Klomfar, M. Součková, A. H. Harvey, Reference Correlations for Thermophysical Properties of Liquid Water at 0.1 MPa, Journal of Physical and Chemical Reference Data 38 (1) (2009) 21. doi:10.1063/1.3043575.

[29] J. W. Arblaster, Thermodynamic Properties of Copper, Journal of Phase Equilibria and Diffusion 36 (5) (2015) 422–444. doi:10.1007/s11669-015-0399-x.

[30] F. Kenfack, M. Bauer, Innovative Phase Change Material (PCM) for Heat Storage for Industrial Applications, Energy Procedia 46 (2014) 310–316. doi:10.1016/j.egypro.2014.01.187.

[31] S. Vidi, H. Mehling, F. Hemberger, T. Haussmann, A. Laube, Round-Robin Test of Paraffin Phase-Change Material, International Journal of Thermophysics (2014) 1–5doi:10.1007/s10765-014-1754-6.
URL http://dx.doi.org/10.1007/s10765-014-1754-6

[32] Rubitherm GmbH, RT28HC Data Sheet.
URL https://www.rubitherm.eu/media/products/datasheets/

[33] Joint Committee for Guides in Metrology, Evaluation of measurement data - Supplement 1 to the "Guide to the expression of uncertainty in measurement": Propagation of distributions using a Monte Carlo method: JCGM 101:2008.

[34] M. Krzywinski, N. Altman, Visualizing samples with box plots, Nature Methods 11 (2) (2014) 119–120. doi:10.1038/nmeth.2813.

[35] M. Solaguren-Beascoa Fernández, J. M. Alegre Calderón, P. M. Bravo Díez, Implementation in MATLAB of the adaptive Monte Carlo method for the evaluation of measurement uncertainties, Accreditation and Quality Assurance 14 (2) (2009) 95–106. doi:10.1007/s00769-008-0475-6.